Ocean Sci. Discuss., 12, 1263–1289, 2015
www.ocean-sci-discuss.net/12/1263/2015/
doi:10.5194/osd-12-1263-2015

Ocean Science
Discussions
Open Access

Multi-objective entropy evolutionary algorithm for marine oil spill detection using cosmo-skymed satellite data

M. Marghany

Geoscience & Digital Earth Center, Research Institute for Sustainability & Environment,
Universiti Teknologi Malaysia, 81310 Skudai, UTM, Johor, Malaysia

Received: 25 April 2015 – Accepted: 1 June 2015 – Published: 25 June 2015

Correspondence to: M. Marghany (magedupm@hotmail.com)

Published by Copernicus Publications on behalf of the European Geosciences Union.

Multi-objective entropy evolutionary algorithm for marine oil spill detection

M. Marghany

Abstract

Oil spill pollution has a substantial role in damaging the marine ecosystem. Oil spill that floats on top of water, as well as decreasing the fauna populations, affects the food chain in the ecosystem. In fact, oil spill is reducing the sunlight penetrates the water, limiting the photosynthesis of marine plants and phytoplankton. Moreover, marine mammals for instance, disclosed to oil spills their insulating capacities are reduced, and so making them more vulnerable to temperature variations and much less buoyant in the seawater. This study has demonstrated a design tool for oil spill detection in SAR satellite data using optimization of Entropy based Multi-Objective Evolutionary Algorithm (E-MMGA) which based on Pareto optimal solutions. The study also shows that optimization entropy based Multi-Objective Evolutionary Algorithm provides an accurate pattern of oil slick in SAR data. This shown by 85 % for oil spill, 10 % look-alike and 5 % for sea roughness using the receiver-operational characteristics (ROC) curve. The E-MMGA also shows excellent performance in SAR data. In conclusion, E-MMGA can be used as optimization for entropy to perform an automatic detection of oil spill in SAR satellite data.

1 Introduction

Lately, oil spills in coastal zones have received much critical anxiety for its great damages on the coastal ecological system. Synthetic aperture radar (SAR) has proved as appropriate sensor for oil spill surveying for its wide-area and all-day all-weather surveillance potentials. Owing to its extraordinary imaging mechanism, conversely, the accuracy of oil spill detection is challenged by multiplicative speckle noise and dark patches instigated by other physical phenomena. In this perspective, dark patches do not be related to oil spills are known as look-alikes. They can be acclaimed to zones of low wind speed, internal waves, biogenic films, grease ice, wind front areas, areas sheltered by land, rain cells, current shear zones and up-welling zones (Lombardini et al.,

OSD
12, 1263–1289, 2015

1989; Teivero et al., 1998; Marghany, 2001). Consequently, three steps are expected to automatically detect oil spills in SAR images: (i) dark spot detection, (ii) dark spot feature extraction, and (iii) dark spot classification. Various classification algorithms for oil spill detection have been utilized, including pattern recognition algorithms (Teivero et al., 1998), spatial frequency spectrum gradient algorithms (Lombardini et al., 1989; Nirchio et al., 2005) and algorithms based on fuzzy and neural networks (Barni et al., 1995; Calabresi et al., 1999; Garcia-Pineda et al., 2013). Consequently, the oil spill automatic detection from SAR data are requested standard algorithm to overwhelm the multiplicative speckle noise and look-alike phenomena appearances. Marghany (2001) introduced entropy algorithm which is based on texture coocurrenace matrix for oil spill automatic detection from RADARSAT-1 SAR data. He found that entropy algorithm is able to discriminate between oil spill and look-alike phenomena. Indeed, the entropy algorithm can support the automatic detection of oil spill by reducing the uncertainty on the basis of information produced by multiplicative speckle noise and look-alike phenomena effects. Further, Shi et al. (2008) have implemented entropy texture algorithm for oil spill detection from SAR and optical remote sensing data. They found that the oil spill pixels are smoother than the surrounding environment. Shi et al. (2008) confirmed the work done by Marghany (2001). Besides, Minchew et al. (2012) declared the variability of the entropy is consistent with the variability of the oil properties suggesting that the entropy is providing a qualitative measure of the oil characteristics. Specifically, when there is open water and a thin sheen, the entropy is close to 0, but in the presence thicker oil (e.g. emulsion) the entropy has values that are close to 1.

Conversely, Skrunes et al. (2012) reported several disadvantages associated with oil spill detection using the current SAR sensors and stated that SAR sensors cannot detect the thickness distribution, volume, oil/water emulsion ratio or chemical properties of an oil slick. Instead, that group recommended the use of multi-polarization observations, i.e., the data acquired by the RADARSAT-2 and TerraSAR-X satellites. In addition, quad-pol RADARSAT-2 SAR (Zhang et al., 2011) can provide information about oil spill thickness compared to other SAR single channel such as RADARSAT-1 SAR, ERS-

OSD
12, 1263–1289, 2015

1/2 and Terra SAR. In this reagrd, range of theoretical polarimetric SAR developments has gradually qualified the accurate distinction between mineral oil slicks and biogenic slicks (Liu et al., 2011; Minchew et al., 2012; Skrunes et al., 2012). Recently, Minchew et al. (2012) used Uninhabited Aerial Vehicle Synthetic Aperture Radar (UAVSAR) L-band polarimetric for retrieving the oil volumetric concentration in a thick slick that is based on Cloude-Pottier entropy algorithm (Cloude and Pottier, 1996). The work of Liu et al. (2011); Minchew et al. (2012); Skrunes et al. (2012) the Cloude-Pottier entropy algorithm (H) ($0 \leq H \leq 1$) can provide a measure of the amount of mixing between scattering mechanisms. For a wind-roughened ocean surface, the scattering is dominated by a single dominant scattering mechanisms, namely Bragg scattering ($H \to 0$). In the presence of an oil slick, however, the entropy increases ($H \to 1$) which is due to the number independent scattering mechanisms increasing due to damping of the small-scale Bragg waves. Nevertheless, in the region between imaging slick-free water and an oil slick, the entropy varied as a function of the properties of the oil (e.g. sheen, emulsion) (Liu et al., 2011; Zhang et al., 2011; Minchew et al., 2012; Skrunes et al., 2012).

Newly, Staples and Rodrigues (2013) stated that entropy cannot be obtained from single co-polarized radar data, but requires quad-polarized data. Quad-polarized data means that the radar acquires two co-polarized channels (HH and VV) and two cross-polarized channels (HV and VH), but equally as important, quad-polarized data are phase-preserving meaning that the inter-channel phase difference (e.g. phase difference between HH and VV) is available. In contrast, Marghany (2001) and Marghany and van Genderen (2014) entropy texture algorithm provides excellent performance for oil spill automatic detection from different single SAR data.

Recently, Marghany (2014) utilized the Genetic algorithm (GA) as automatic detection algorithm for oil spill in RADARSAT-2 SAR data. Marghany (2014a) confirmed the work of Topouzelis et al. (2009). Both studies have agreed that the genetic algorithm is able to extract oil spill footprint boundaries automatically from the surrounding pixels without using a separate segmentation algorithm, as was done by Skrunes

OSD
12, 1263–1289, 2015

et al. (2012). Consistent with Marghany (2014), the genetic algorithm has the ability to determine the optimal number of regions of oil spill segmentation or to choose certain features, i.e., the size of the analysis window or selected heuristic thresholds. Further, The GA is shown to be able to identify and remove pixels that do not significantly contribute to oil slick footprint in SAR data. This conclusion has approved the findings of Mohanta and Sethi (2012).

The novelty of this work is designing optimization tool for the real time oil spill automatic detection using Entropy-Based Multi-objective Evolutionary Algorithm without involving others tool such as neural network or any image processing classification tools. Indeed, previous studies have executed artificial neural networks (Topouzelis et al., 2009; Mohanta and Sethi, 2012) or post-classification techniques (Barni et al., 1995; Calabresi et al., 1999), which are considered to be semi-automatic techniques (Marghany, 2001). Furthermore, both artificial neural networks and post-classification techniques are time-consuming and the probability of misclassification does not always decrease as the number of features increases, especially when sample data are insufficient.

Incidentally, the main objective of this work is to minimalize the look-alike dark pixels for accurate oil spill automatic detection in COSMO-SkyMed SAR satellite data which could be involved with oil spill footprint was detected by entropy and genetic algorithm. The Entropy-Based Multi-objective Evolutionary Algorithm uses both basic and advanced operators. For illustrative purposes, the method has been operated to oil spill footprint boundaries shape optimization which allows local and global optimizations. Indeed, global optimization which involves finding the optimal oil spill boundary shapes in COSMO-SkyMed data. Look-alike pixels can be removed to reach the optimal oil spill automatic shape detection.

OSD
12, 1263–1289, 2015

2 Entropy algorithms

This section describes the main equations of entropy algorithm and entropy-based multi-objective Evolutionary Algorithm (E-MMGA). These two algorithms are used for detection of oil spill from observed SAR satellite images.

2.1 Entropy co-occurrence algorithm

Be a consequence of Harmancioglu (1981), entropy is a quantitative compute of the information content of a series of data since reduction of uncertainty, by making observations, equals the same amount of gain in information. Therefore, Marghany (2001) and Marghany and van Genderen, (2014) stated that entropy is a measure of the degree of uncertainty of random oil spill footprint discrimination. In a definition adopted from information theory (Cloude and Pottier, 1996), entropy is the numerical expression of oil spill footprint boundaries in SAR images. In using this concept, oil spill footprint can be measured indirectly based on the degree of the reduction of multiplicative speckle noises and uncertainty of look-alike effects. The main hypothesis is the oil spill footprint boundaries have larger entropy compared to surrounding environment. Hence, in order to quantitatively assess the cumulative effect of uncertainty in oil spill footprint, entropy can be used as a metric for population diversity of oil spill footprint boundaries which are stored at each intersection of the column j and row i of the various slick areas. At the rear of Amorocho and Espildora, (1973) and Harmancioglu (1981); Magrghany and van Genderen (2014), the uncertainty (C) associated with the oil spill pixel value of x_i for a random variable X is then written as

$$C(x_i) = \ln(p(x_i))^{-1} \quad (1)$$

where p_i is the probability distribution of $X_1 = \{x_i\}$ and i is represented raw. The expected value of all of the entropy (E) is adapted from Harmancioglu (1981) which can

OSD
12, 1263–1289, 2015

correlated with the random variable X by the following expression:

$$E(X) = \sum_i p(x_i)\ln(p(x_i))^{-1} \tag{2}$$

Equations (1) and (2) are expressed the probability of oil spill footprint boundaries and its entropy in raw i. Therefore, Eq. (2) can be given in two directions of raw i and column j, then the two dimensional entropy $E(X,Y)$ is given as

$$E(X,Y) = \sum_j \left[\sum_i p(x_i,y_j)\ln(p(x_i,y_j))^{-1}\right] \tag{3}$$

Equation (3), in other words, represents the joint uncertainty associated with oil spill footprint boundaries in two dimensional of SAR images. It is assumed that the random variables of oil spill and look-alikes footprint boundaries are independent then Eq. (3) can extend as

$$E(X,Y) = \sum_j \left[\sum_i p(x_i)p(y_j)\ln(p(x_i)^{-1}p(y_j)^{-1})\right] \tag{4}$$

Equation (4) can be extended to an n-dimensional vector of independently distributed of oil spill and look-alikes footprint boundaries random variables in SAR data. Hence, in this case, the entropy $E(Z)$ is sum of all of the individual SAR pixel entropies $E(X_i)$ and can be expressed as

$$E(Z) = \sum_j^n E(X_i) \tag{5}$$

In the case of a uniform distribution of given oil spill or look-alikes footprint boundaries, the entropy of given probability $p(x_i) = N^{-1}$ of the number (N) of homogenous

OSD
12, 1263–1289, 2015

Multi-objective entropy evolutionary algorithm for marine oil spill detection

M. Marghany

clustering of the features can be calculated (Chapman, 1986) as

$$E(Z) = \sum_{i=1}^{N} \frac{\ln(N)}{N} \tag{6}$$

The number of features (n) in the solution SAR image space can be estimated based on the upper bound on the joint entropy $E_u(Z)$ for oil spill or look-alikes footprint boundary population as

$$E_u(Z) = n \ln(N) \tag{7}$$

Based on Eqs. (6) and (7) the entropy metric is bounded by

$$0 \le E(Z) \le E_u(Z) \tag{8}$$

Based on Eq. (8), the final entropy metric expression can by written by combination of Eqs. (6) and (7) as follows:

$$0 \le \sum_{j=1}^{n} \left[\sum_{i=1}^{N} p(\beta_{i,j}) \ln \left(p(\beta_{i,j})^{-1} \right) \right] \le n \ln(N) \tag{9}$$

where $p(\beta_{i,j})$ is probability distribution for oil spill footprint backscatter ($\beta_{i,j}$) in raw and column of SAR data. If ($\beta_{i,j}$) is stated as the continuous oil spill backscatter variations that stick to the probability density function of $f(\beta_{i,j})$, the conditional entropy can be expressed in the form of conditional probability density function $f(\beta_1|\beta_2)$ of two given continuous random variants of radar backscatter (β_1) and (β_2). Thus the concept of conditional probability density function $f(\beta_1|\beta_2)$ (Chapman, 1986) can be estimated by

$$E(\beta_1|\beta_2) = -\int_{-\infty}^{+\infty}\int_{-\infty}^{+\infty} f(\beta_1,\beta_2) \ln f((\beta_1|\beta_2) \mathrm{d}\beta_1 \mathrm{d}\beta_2 \tag{10}$$

OSD
12, 1263–1289, 2015

Multi-objective entropy evolutionary algorithm for marine oil spill detection

M. Marghany

where $d\beta_1 d\beta_2$ the interval change of oil spill and look-alikes footprint backscatter, respectively.

Marghany (2001); Staples and Rodrigues (2013); and Marghany and van Genderen (2014) have proved the efficiency and validity of the entropy on oil spill detection in SAR data. Nonetheless, this approach is required range of threshold procedures to discriminate between oil spill footprint quantities and surrounding environment. As a result, the multiplicative speckle noises are not totally vanished around the boundary of oil spill footprints. In this prospective, multi-objective optimization algorithm can involve in entropy metric (Gunawan et al., 2004) to preserve the diversity among different solution to minimize the influence of the look-alikes and multiplicative speckle noise (Lathi, 1968; Marghany, 2001; Zhang et al., 2013).

2.2 Entropy-Based Multi-objective Evolutionary Algorithm (E-MMGA)

Take the advantage of E-MMGA of preserving the diversity of solution set (Gunawan et al., 2004) and solving the multidisciplinary of uncertainty of random oil spill footprint discrimination in SAR data. The uniqueness of this study is to deal with entropy of oil spill detection as multi-objective Genetic Algorithm (GA). Comprehending Coello et al. (2002), the multi-objective optimization (MOP) has already been successfully adopted to solve uncertainty of object detection in SAR images (Marghany, 2014a). In general, MOP consists of n decision variable parameters, k objective functions and m constraints (Gunawan et al., 2004). Multi-objective Optimization (Marghany, 2014b; Gunawan et al., 2004) aims at conducting optimization for a range of functions as follows

$$\text{minimize } \boldsymbol{F} = (f_1(\beta), f_2(\beta), \ldots, f_m(\beta))^T \tag{11}$$

$$\text{Subject to } E(\beta_1|\beta_2) \in I \in \Omega \tag{12}$$

where I is SAR data and Ω is the definition domain of functions or the feasible region in decision space. In this research, two objectives are considered. One is oil spill

OSD
12, 1263–1289, 2015

Multi-objective entropy evolutionary algorithm for marine oil spill detection

M. Marghany

backscatter and the other is sea surface, ship, lookalikes, and land backscatters. The definitions of entropy of oil spill and non-oil spill footprint boundaries are given as follows:

1. Entropy of oil spill footprint boundaries ($E(\beta_{max})$): the variation of maximum entropy $E(\beta_{max})$ which contain oil spill footprint boundaries i.e. $E(\beta_{max}) = \max\{E(\beta_1, \beta_2, \ldots, \beta_k)\}$. Where $E(\beta_{ij})$ denotes the entropy of oil spill boundaries in i and j directions $i, j, \forall i, j = 1, 2, \ldots, k$.

2. Total of entropy of oil spill footprint boundaries is ($\sum E(\beta_{ij})$): the sum of entropy of the surrounding oil spill environment in SAR data. Then the Pareto optimal solutions are applied to retain the discrimination of oil spills entropy diversity and surrounding entropy environment.

Let $E(\beta_0, \beta_1, \beta_2) \in E(\beta_{SAR})$, and $E(\beta_{SAR})$ is a feasible entropy in whole SAR image. And β_0 is called the Pareto optimal solution in the minimization problem for identification of oil spill pixels. if the following conditions are satisfied (Marghany, 2014b).

1. If $f(E(\beta_1))$ is said to be partially greater than $f(E(\beta_2))$, i.e. $f_i(E(\beta_1) \geq f_i(E(\beta_2))$, $\forall\, i = 1, 2, \ldots, n$ and $f_i(E(\beta_1)) > f_i(E(\beta_2))$, $\exists\, i = 1, 2, \ldots, n$. Then $E(\beta_1)$ is said to be dominated by $(E(\beta_2)$.

2. If there is no $E(\beta) \in E(\beta_{SAR})$ s.t. $E(\beta)$ dominates $E(\beta_0)$, then $E(\beta_0)$ is the Pareto optimal solutions for identifying entropy of oil spill footprint boundaries $E(\beta_{max})$.

Following Marghany (2014b), the optimization of oil spill detection from SAR data using entropy based MOEA E-MOEA, the entropy of oil spill footprint boundaries must be coded into a Genetic Algorithm syntax form i.e. the chromosome form. In this problem, the chromosome consists of a number of genes where every gene corresponds to a coefficient in the nth-order surface fitting polynomial as given by

$$f(i, j) = E(\beta_0 + \beta_1 i + \beta_2 j + \beta_3 i^2 + \beta_4 ij + \beta_5 j^2 + \ldots + \beta_m j^n) \quad (13)$$

OSD
12, 1263–1289, 2015

Multi-objective entropy evolutionary algorithm for marine oil spill detection

M. Marghany

where $E(\beta)[0,1\ldots m]$ are the entropy parameter coefficients that will be estimated by the genetic algorithm to approximate the minimum error for entropy of oil spill discrimination from surrounding environment. i and j are indices of the pixel location in the image respectively, m is the number of coefficients (Fig. 1).

Then the weighted sum to combine entropy of multiple objectives into single objective is given by Zhou et al. (2006).

$$f(E(\beta)) = w_1 f_1(E(\beta)) + w_2 f_2(E(\beta)) + \cdots + w_n f_n((E\beta)) \tag{14}$$

where $f_1(E(\beta)), f_2(E(\beta)), \ldots, f_n(E(\beta))$ are the objective functions and $w_1, w_2, \ldots, w_n$ are the weights of corresponding objectives that satisfy the following conditions.

$$\begin{aligned} & w_i \geq 0 \ \forall i = 1,2,\ldots,n \\ & w_1 + w_2 + \ldots + w_n = 1 \end{aligned} \tag{15}$$

Once the weights are determined, the searching direction is fixed. To search Pareto optimal solutions as much as possible, the searching directions should be changed again and again to sweep over the whole solution space. Therefore the weights have to be changed again and again. The weights consist of random numbers and they are generated as the following way (Marghany, 2014b):

$$w_i = \frac{r_i}{r_1 + r_2 + \ldots + r_n}, \quad \forall i = 1,2,\ldots,n \tag{16}$$

where $r_1, r_2, \ldots, r_n$ are random numbers within (0, 1). Solutions searched through changing directions are collected in a set. Then the definition of Pareto optimal solution is applied to determine which solutions in the set are Pareto optimal. The step repeats in every generation in E-MOGA.

To determine the diversity of entropy of multi-objectives which is mostly more than two objectives for instance, oil spill, look-alikes, rough sea, and low wind zone, compute the distance from a given footprint centre to its nearest neighbour boundaries. This

OSD
12, 1263–1289, 2015

can be computed by following equation adopted from Zhou et al. (2006) and Zhang et al. (2013).

$$\Psi = \sum_{k=1}^{m} d(E(\beta_{ij})\Omega) + \sum_{l\in\Omega} \left| d(l,\Omega) - \overline{d} \right| \times \left[\sum_{k=1}^{m} d(E(\beta_{ij}),\Omega) + (|\Omega - m|)\overline{d} \right]^{-1} \tag{17}$$

There are m solutions $E(\beta_1),...,E(\beta_m)$ sorted by an objective in SAR space data, $d_1,...,d_{m-1}$ are the edge distances between adjacent different oil spill and look-alike footprint boundaries and Ω is set of solutions regarding oil spill or look-alikes footprint boundaries, and

$$d(E(\beta_1),\Omega) = \min_{E(\beta_j)\in\Omega, E(\beta_j)\neq E(\beta_i)} \left\| F(E(\beta_i)) - F(E(\beta_j)) \right\| \tag{18}$$

$$d = |\Omega|^{-1} \sum_{E(\beta)\in\Omega} d(E(\beta),\Omega). \tag{19}$$

E-MMGA is run until there is no further improvement in the entropy value (i.e., entropy is maximum), and then it is stopped. The solution of the overall problem is obtained by taking the nondominated frontier of the points in the grand pool of the last E-MMGA (Marghany, 2014b) iteration (Zhang et al., 2013).

3 Results and discussion

In this study, COSMO-SkyMed image is acquired on 29 July 2010 at 11:23:33 UTC which is implemented for oil spill detection in the Koh Samet island, Thailand. This data covered 12°31′48″ to 12°37′48″ N latitude and 101°2′24″ to 101°33′37″ E longitude (Fig. 2). According to Marghany (2014b), the oil spill has moved away from the mainland and has started to disperse to an extent. However, what is worrying now is that it seems to have reached a group of islands dominated by Koh Kudee. The stag-horn and giant clam coral reef is dominated natural features of Koh Samet island (Fig. 2b) with water depth less than 20 m depth.

OSD
12, 1263–1289, 2015

The Satellite has a Synthetic Aperture Radar (SAR) with multiple polarization modes, including a fully polarimetric mode in which HH, HV, VV and VH polarized data are acquired. Its meduim resolution is 5 m in Stripmap with the maximum coverage is 40 km × 40 km, geometric resolution is 25 m^2, pixel spacing is 0.5 m × 0.5 m, and the incident angle is between 20 to 59° with VV polarization (Table 1). Figure 3 shows the COSMO-SkyMed data where the oil spill is heading by 16.5° towards inland within 6.59 km length of the island to inland (Fig. 3).

Figure 4 shows the variation in the average backscatter intensity along the oil slick footprint. The average backscatter intensity was damped by −20 to −9 dB and decreased over time as the oil slick footprint gradually increased (Fig. 4). Besides, the sea surface roughness has highest backscatter values of −10 dB than oil spill footprint pixels. Consistent with and Trivero et al. (2007) and Marghany (2014b), oil spill changes the roughness of the ocean surface to smoothness surface in which appears as dark footprint as compared to the surrounding ocean (Lombardini et al., 1989; Trivero et al., 1998; Nirchio et al., 2005; Zhang et al., 2011). Consequently, the speckle caused obstacles in dark footprint identifications in SAR data (Marghany, 2001; Skrunes et al., 2012). Additional, the wind speed is recorded in 29 July 2013 was ranged between 1 to 7 m s^{-1}. Besides, the measured reductions of backscattered radar power at X-band could be impacted by instrumental limitations, i.e. by the fact that the backscattered radar power reaches the noise floor (Trivero et al., 2007; Marghany, 2014b).

Figure 5 shows the entropy algorithm result. Clearly, the oil spill footprint has lower entropy value of 1.5 as compared to sea roughness and land. The land has highest entropy value of 3.5 entropy and sea roughness has entropy value of 2.7. Indeed, non-Bragg scattering is existing on land as backscatter becomes depolarized (Shi et al., 2008; Skrunes et al., 2012). Additionally, entropy algorithm has identified oil spill footprint boundaries by entropy value of 3.3. However, land entropy and oil spill footprint boundary having close entropy. In fact, entropy represents the randomness of scattering mechanism (Shi et al., 2008). According to Marghany (2001); Fukunaga

OSD
12, 1263–1289, 2015

(2013); and Marghany and van Genderen (2014) entropy is measure of uniformity in SAR image. In general, the entropy is a measure of variability or randomness because the concentration of the backscatter changes in relatively few locations would be non-random essentially. This confirms the study done by Shi et al. (2008).

Figure 6 shows the output result of E-MMGA. Clearly, E-MMGA is able to produce four different segmentation boundaries. Besides Fig. 7 shows that the thick oil spill footprint has highest E-MMGA value of 2 than medium and light oil spill. This is mainly because each multi-objective function in E-MMGA tends to bias its population towards the extreme edges of the Pareto frontier. This is confirms the work was done by Gunawan et al. (2004). Compared to entropy algorithm, E-MMGA is able to identify the look-alike footprint boundaries and discriminate accurately between, oil spill and look-alike, and surrounding sea surface. E-MMGA can accurately identify the morphological boundary of oil spill and assigned by different segmentation layer in COSMO-SkyMed satellite data. In fact, the Entropy-Multi-Objective Evolutionary Genetic Algorithm (E-MMGA) provides a set of compromised solutions called Pareto optimal solution since no single solution can optimize each of the objectives separately. The decision maker is provided with the set of Pareto optimal solutions in order to choose solution based on the decision maker's criteria. This sort of E-MMGA solution technique is called a posteriori method since decision is taken after searching is finished. This confirms the work done by Coello et al. (2002). In this context, the Pareto-optimization approach does not require any a priori preference decisions between the conflicting of oil spill, look-alike, land, and surrounding sea footprint boundaries. Further, Pareto-optimal points have form Pareto-front as shown in Fig. 6 in the multi-objectives function of the COSMO-SkyMed data space.

Entropy-Multi-Objectives Evaluation Genetic Algorithm (E-MMGA) which based on the Pareto optimal solutions provides excellent discrimination of oil spill footprint boundaries. This can be confirmed by the receiver-operator characteristics (ROC) curve (Fig. 8). In this regard, the existing of weight sum of objective function converts a conflicting multiobjective problem of oil spill and surrounding sea feature objectives. This

OSD
12, 1263–1289, 2015

can be seen in ROC curve where oil spill has an area difference of 85 % which is larger than look-alike and sea surface areas. Further, p probability of 0.0005 another proof for excellent of E-MMGA for oil spill detection. This study shows a great performance as compared to previous work done by Marghany (2001) Shi et al. (2008); Marghany (2014a and b). This because of Pareto-front contains the Pareto-optimal solutions and in case of continuous front, it divides the pixels objective function space into two parts, which are non-optimal solutions and infeasible solutions. In this regard, it improved the robustness of pattern search and improved the convergence speed of MOEA. This confirms the work of Zhang et al. (2013).

On the word of Gunawan et al.,(2004), E-MMGA is able to preserve diversity and converge as fast as most of the single-level approaches (which are expected to be more efficient but less practical for large-scale problems of multidisciplinary nature). Besides, it improves overall quality of solutions by explicitly optimizing the entropy index at every system-level iteration, and then using this information to bias the search process toward obtaining a solution set with maximum diversity.

4 Conclusions

This study has demonstrated work to optimize the oil spill footprint detection in synthetic aperture radar (SAR) data. Therefore, Entropy-based Multi-objective Evolutionary Algorithm (E-MMGA) has implemented with COSMO-SkyMed data during the oil spill event along the coastal water of along Koh Samet island, Thailand. Besides, Pareto optimal solution is implemented with E-MMGA to minimize the difficulties of oil spill footprint boundary detection because of the existence of look-alike in SAR data. The study shows that the implementation of Pareto optimal solution and weight sum in E-MMGA generated accurate pattern of oil slick. Furthermore, thick oil spill has highest value of 2 E-MMGA than thin and medium spills. The E-MMGA, is able to preserve the morphology of oil spill footprint boundaries i.e. thick, medium, and light. In addition, the receive-operational characteristics (ROC) curve confirmed accurately performance

OSD
12, 1263–1289, 2015

of E-MMGA with 85 % oil spill detection, 10 % for look-alike and 5 % for surrounding sea surface boundary identification. In conclusion, E-MMGA is considered as excellent algorithm to discriminate oil spill from look-alikes and also to identify thick oil spill from thin one.

Acknowledgements. The author would like to thank Geo-informatics and Space Technology Development Agency (GISTDA) of Thailand for providing COSMO-SkyMed data

References

Amorocho, J. and Espildora, B.: Entropy in the assessment of uncertainty in hydrologic systems and models, Water Resour. Res., 9, 1511–1522, 1973.

Barni, M., Betti, M., and Mecocci, A.: A fuzzy approach to oil spill detection an SAR images, International Geoscience and Remote Sensing Symposium, 1995, IGARSS'95, "Quantitative Remote Sensing for Science and Applications", 157–159, 1995.

Calabresi, G., Del Frate, F., Lichtenegger, J., Petrocchi, A., and Trivero, P.: Neural networks for the oil spill detection using ERS-SAR data, IEEE 1999 International Geoscience and Remote Sensing Symposium, 1999, IGARSS'99 Proceedings, 215–217, 1999.

Chapman, T. G.: Entropy as a measure of hydrologic data uncertainty and model performance, J. Hydrol., 85, 111–126, 1986.

Cloude, S. R. and Pottier, E.: A review of target decomposition theorems in radar polarimetry, IEEE T. Geosci. Remote, 34, 498–518, 1996.

Coello, C. A. C., Van Veldhuizen, D. A., and Lamont, G. B.: Evolutionary Algorithms for Solving Multi-Objective Problems, Springer, 2002.

Fukunaga, K.: Introduction to Statistical Pattern Recognition, Academic Press, 2013.

Garcia-Pineda, O., MacDonald, I. R., Li, X., Jackson, C. R., and Pichel, W. G.: Oil spill mapping and measurement in the Gulf of Mexico with Textural Classifier Neural Network Algorithm (TCNNA), IEEE J. Sel. Top. Appl., 6, 2517–2525, 2013.

Gunawan, S., Farhang-Mehr, A., and Azarm, S.: On maximizing solution diversity in a multiobjective multidisciplinary genetic algorithm for design optimization, 2004.

Harmancioglu, N.: Measuring the information content of hydrological processes by the entropy concept, Centennial of Ataturk's Birth, Journal of the Civil Engineering Faculty of Ege University, 12, 13–88, 1981.
Lathi, B. P.: An introduction to random signals and communication theory, 1968.
Liu, P., Li, X., Qu, J. J., Wang, W., Zhao, C., and Pichel, W.: Oil spill detection with fully polarimetric UAVSAR data, Mar. Pollut. Bull., 62, 2611–2618, 2011.
Lombardini, P., Fiscella, B., Trivero, P., Cappa, C., and Garrett, W.: Modulation of the spectra of short gravity waves by sea surface films: slick detection and characterization with a microwave probe, J. Atmos. Ocean. Tech., 6, 882–890, 1989.
Marghany, M.: Utilization of a genetic algorithm for the automatic detection of oil spill from RADARSAT-2 SAR satellite data, Mar. Pollut. Bull., 89, 20–29, 2014a.
Marghany, M.: Multi-objective evolutionary algorithm for oil spill detection from COSMO-SkeyMed satellite, in: Computational Science and Its Applications–ICCSA 2014, Springer, 355–371, 2014b.
Marghany, M. and van Genderen, J.: Entropy algorithm for automatic detection of oil spill from radarsat-2 SAR data, IOP Conference Series: Earth and Environmental Science, 012051, 2014.
Minchew, B., Jones, C. E., and Holt, B.: Polarimetric analysis of backscatter from the Deepwater Horizon oil spill using L-band synthetic aperture radar, IEEE T. Geosci. Remote, 50, 3812–3830, 2012.
Mohanta, R. K. and Sethi, B.: A review of genetic algorithm application for image segmentation, International Journal of Computer Technology & Applications, 3, 720–723, 2012.
Nirchio, F., Sorgente, M., Giancaspro, A., Biamino, W., Parisato, E., Ravera, R., and Trivero, P.: Automatic detection of oil spills from SAR images, Int. J. Remote Sens., 26, 1157–1174, 2005.
Shi, L., Zhao, C., Fan, K., Shi, Y., and Liu, P.: Texture feature application in oil spill detection by satellite data, Congress on Image and Signal Processing, 2008, CISP'08, 784–788, 2008.
Skrunes, S., Brekke, C., and Eltoft, T.: An experimental study on oil spill characterization by multi-polarization SAR, 9th European Conference on Synthetic Aperture Radar, 2012, EUSAR, 139–142, 2012.
Staples, G. and Rodrigues, D. F.: Maritime environmental surveillance with RADARSAT-2, Anais XVI Simpósio Brasileiro de Sensoriamento Remoto – SBSR, Foz do Iguaçu, PR, Brasil, 13–18 april 2013, INPE, available at: http://www.dsr.inpe.br/sbsr2013/files/p1061.pdf, 2013.

OSD
12, 1263–1289, 2015

Multi-objective entropy evolutionary algorithm for marine oil spill detection

M. Marghany

Topouzelis, K., Stathakis, D., and Karathanassi, V.: Investigation of genetic algorithms contribution to feature selection for oil spill detection, Int. J. Remote Sens., 30, 611–625, 2009.
Trivero, P., Fiscella, B., Gomez, F., and Pavese, P.: SAR detection and characterization of sea surface slicks, Int. J. Remote Sens., 19, 543–548, 1998.
Trivero, P., Biamino, W., and Nirchio, F.: High resolution COSMO-SkyMed SAR images for oil spills automatic detection, IEEE International Geoscience and Remote Sensing Symposium, 2007, IGARSS 2007, 2–5, 2007.
Zhang, B., Perrie, W., Li, X., and Pichel, W. G.: Mapping sea surface oil slicks using RADARSAT-2 quad-polarization SAR image, Geophys. Res. Lett., 38, 1–5, doi:10.1029/2011GL047013, 2011.
Zhang, Y., Wang, S., Ji, G., and Dong, Z.: Genetic pattern search and its application to brain image classification, Math. Probl. Eng., 1–8, doi:10.1155/2013/580876, 2013.
Zhou, A., Jin, Y., Zhang, Q., Sendhoff, B., and Tsang, E.: Combining model-based and genetics-based offspring generation for multi-objective optimization using a convergence criterion, IEEE Congress on Evolutionary Computation, 2006, CEC 2006, 892–899, 2006.

OSD
12, 1263–1289, 2015

Multi-objective entropy evolutionary algorithm for marine oil spill detection

M. Marghany

OSD
12, 1263–1289, 2015

Multi-objective entropy evolutionary algorithm for marine oil spill detection

M. Marghany

Table 1. Characteristics of COSMO-SkyMed used.

Mode	Resolution (m)	Polarization
Stripmap	5 × 5	VV

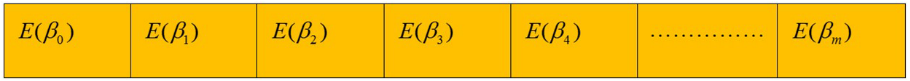

Figure 1. Coding scheme of the coefficients of the *n*th-order surface fitting polynomial into the chromosome syntax form.

OSD
12, 1263–1289, 2015

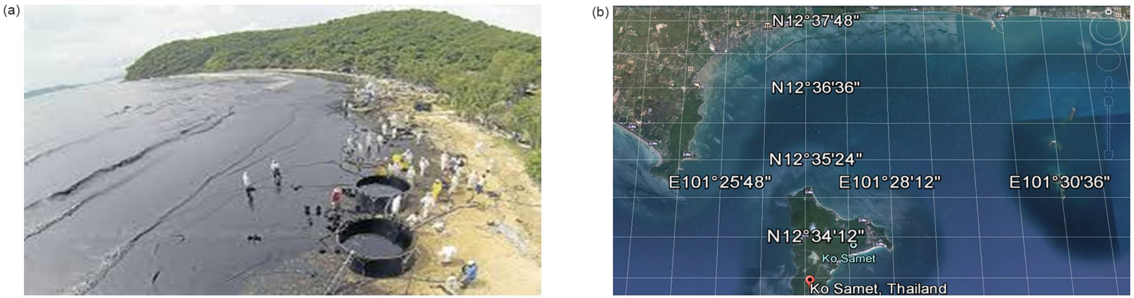

Figure 2. Oil spill covers beach of **(a)** Koh Samet Island and **(b)** Google map of Koh Samet Island.

OSD
12, 1263–1289, 2015

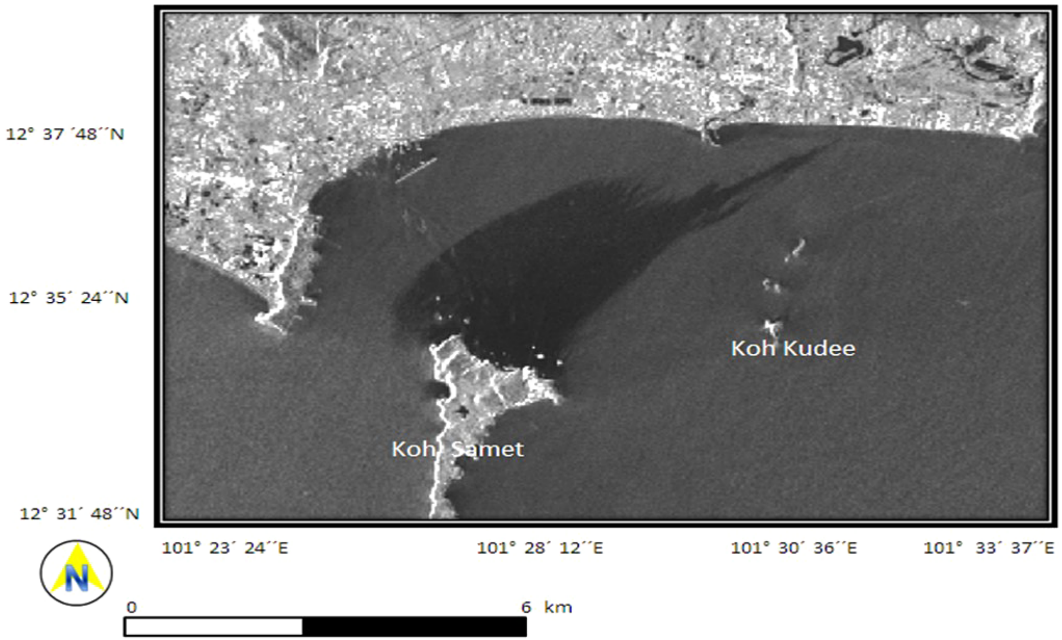

Figure 3. COSMO-SkyMed data along Koh Samet island, Thailand.

OSD
12, 1263–1289, 2015

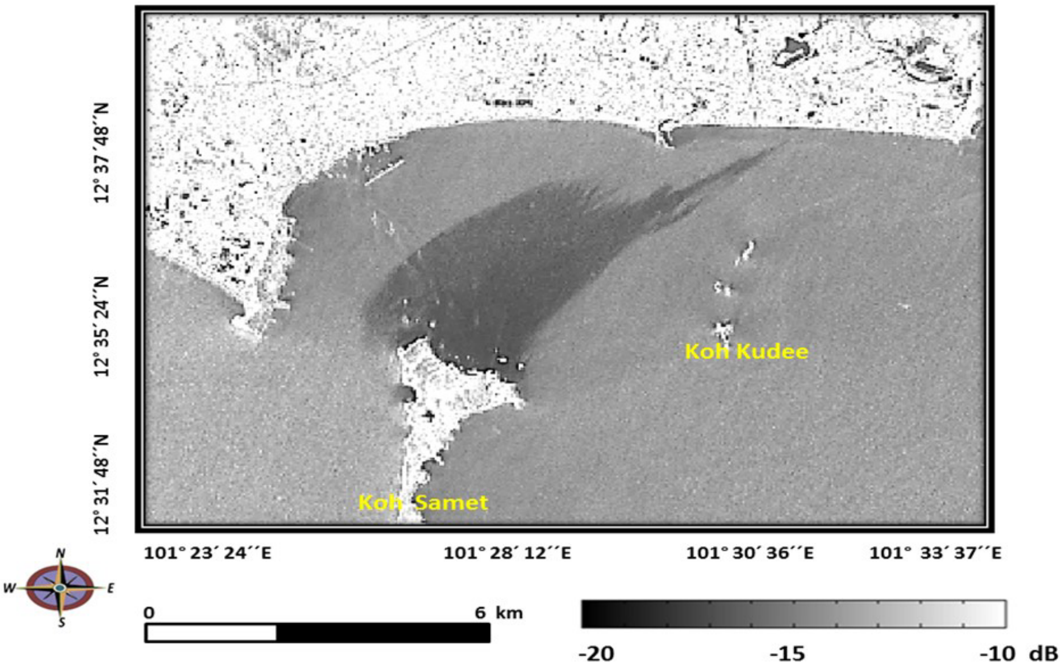

Figure 4. Average backscatter variations in COSMO-SkyMed.

OSD
12, 1263–1289, 2015

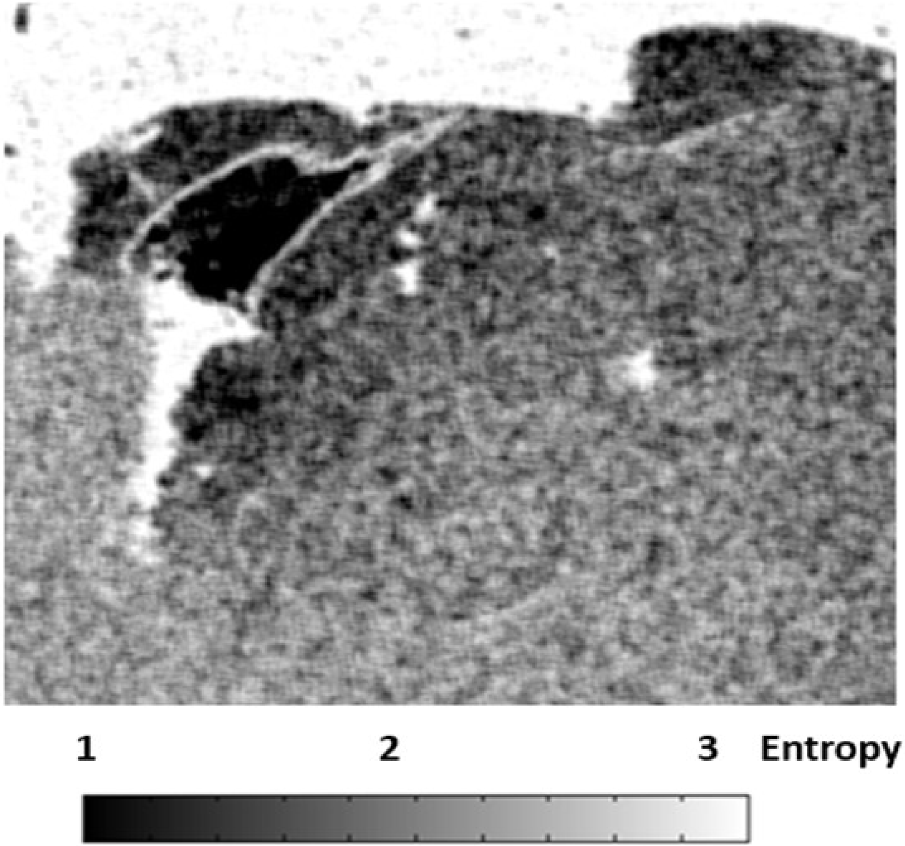

Figure 5. Entropy result for oil spill footprint.

OSD
12, 1263–1289, 2015

Multi-objective entropy evolutionary algorithm for marine oil spill detection

M. Marghany

Title Page
Abstract Introduction
Conclusions References
Tables Figures
◀◀ ▶▶
◀ ▶
Back Close
Full Screen / Esc
Printer-friendly Version
Interactive Discussion

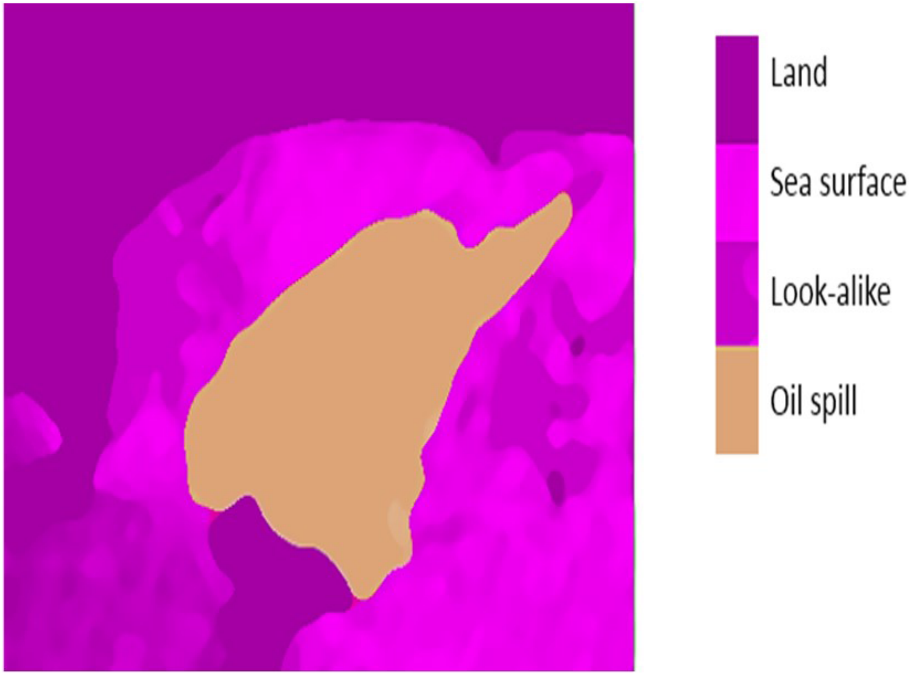

Figure 6. E-MMGA solution for oil spill discrimination in COSMO-SkyMed.

OSD
12, 1263–1289, 2015

Multi-objective entropy evolutionary algorithm for marine oil spill detection

M. Marghany

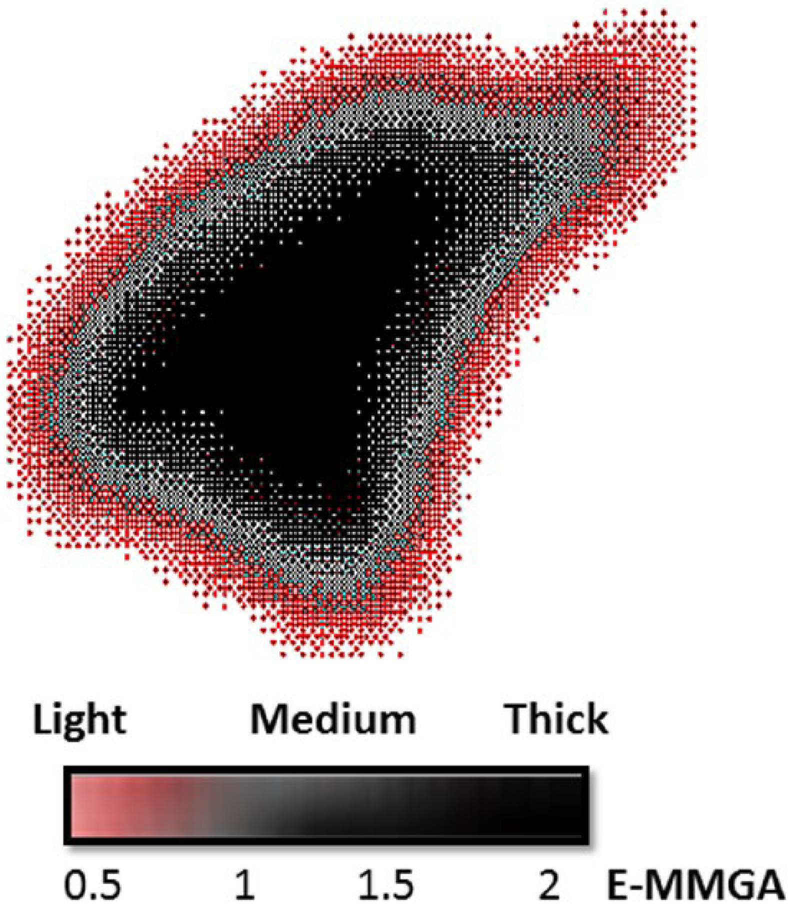

Figure 7. Oil spill footprint Category by E-MMGA.

OSD
12, 1263–1289, 2015

Multi-objective entropy evolutionary algorithm for marine oil spill detection

M. Marghany

Title Page
Abstract Introduction
Conclusions References
Tables Figures
Back Close
Full Screen / Esc
Printer-friendly Version
Interactive Discussion

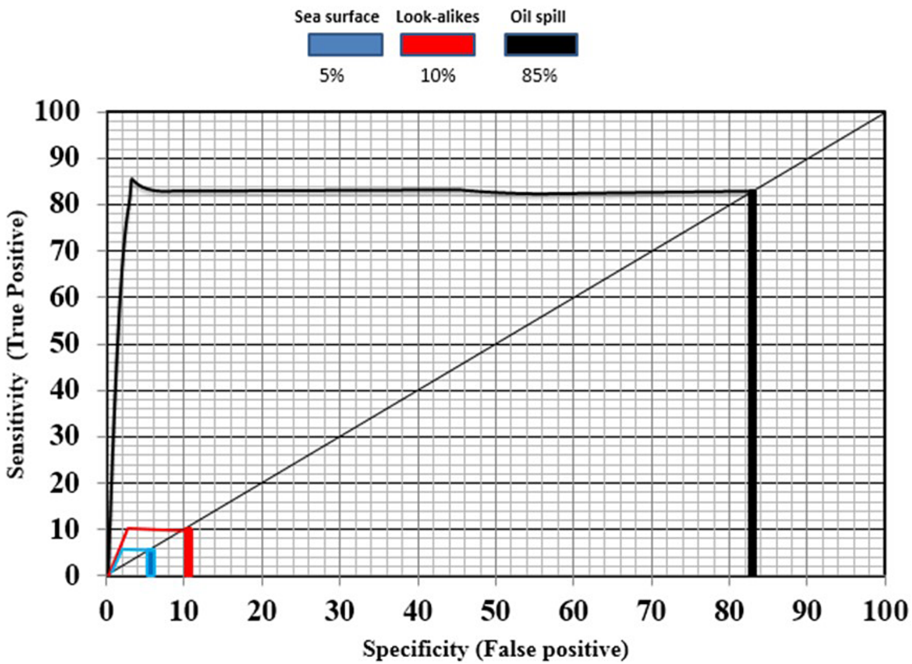

Figure 8. ROC for oil spill discrimination using E-MMGA.

OSD
12, 1263–1289, 2015

Multi-objective entropy evolutionary algorithm for marine oil spill detection

M. Marghany